HHS Public Access

Author manuscript

Nat Genet. Author manuscript; available in PMC 2012 October 01.

Published in final edited form as:

Nat Genet. ; 44(4): 450–S2. doi:10.1038/ng.1103.

Mutations affecting the cytoplasmic functions of the co-chaperone DNAJB6 cause limb-girdle muscular dystrophy

Jaakko Sarparanta[1,13], **Per Harald Jonson**[1,13], **Christelle Golzio**[2,13], **Satu Sandell**[3,4], **Helena Luque**[1], **Mark Screen**[1], **Kristin McDonald**[5,6], **Jeffrey M. Stajich**[5], **Ibrahim Mahjneh**[7,8], **Anna Vihola**[1], **Olayinka Raheem**[3], **Sini Penttilä**[3], **Sara Lehtinen**[1], **Sanna Huovinen**[3,9], **Johanna Palmio**[3], **Giorgio Tasca**[10], **Enzo Ricci**[11], **Peter Hackman**[1], **Michael Hauser**[5,6], **Nicholas Katsanis**[2], and **Bjarne Udd**[1,3,12]

[1]Folkhälsan Institute of Genetics and Department of Medical Genetics, Haartman Institute, University of Helsinki, Helsinki, Finland [2]Center for Human Disease Modeling, Duke University Medical Center, Durham, North Carolina, USA [3]Neuromuscular Research Unit, Department of Neurology, University Hospital and University of Tampere, Tampere, Finland [4]Department of Neurology, Seinäjoki Central Hospital, Seinäjoki, Finland [5]Department of Medicine, Duke University Medical Center, Durham, North Carolina, USA [6]Center for Human Genetics, Duke University Medical Center, Durham, North Carolina, USA [7]Department of Neurology, Pietarsaari Hospital, Pietarsaari, Finland [8]Department of Neurology, University of Oulu, Oulu, Finland [9]Department of Pathology, University Hospital and University of Tampere, Tampere, Finland [10]Don Carlo Gnocchi Onlus Foundation, Milan, Italy [11]Institute of Neurology, Catholic University School of Medicine, Rome, Italy [12]Department of Neurology, Vaasa Central Hospital, Vaasa, Finland

Abstract

Limb-girdle muscular dystrophy type 1D (*LGMD1D*) was linked to 7q36 over a decade ago[1], but its genetic cause has remained elusive. We have studied nine LGMD families from Finland, the U.S., and Italy, and identified four dominant missense mutations leading to p.Phe93Leu or p.Phe89Ile changes in the ubiquitously expressed co-chaperone DNAJB6. Functional testing *in vivo* showed that the mutations have a dominant toxic effect mediated specifically by the cytoplasmic isoform of DNAJB6. *In vitro* studies demonstrated that the mutations increase the half-life of DNAJB6, extending this effect to the wild-type protein, and reduce its protective anti-aggregation effect. Further, we show that DNAJB6 interacts with members of the CASA complex, including the myofibrillar-myopathy-causing protein BAG3. Our data provide the genetic cause of LGMD1D, suggest that the pathogenesis is mediated by defective chaperone function, and

Correspondence should be addressed to B.U. (bjarne.udd@netikka.fi).

[13]These authors contributed equally to this work

Author contributions J.S., P.H.J., C.G., M.H., N.K. and B.U. wrote and all authors approved and commented on the paper; B.U., S.S., J.M.S., J.P., G.T., E.R. and I.M. recruited and evaluated the patients; H.L., S.L., K.M., S.P. and P.H. did the genetic analysis of patients; M.S. and P.H. did the transcript analysis; C.G., H.L., K.M. and J.S. made the plasmid constructs; C.G. performed the zebrafish studies and protein stability assays; O.R., S.H., A.V. and J.S. performed microscopy of patient muscle samples; S.H. did electron microscopy; J.S., P.H.J. and H. L. performed the FTA, oligomerization, and CASA interaction studies.

highlight how mutations expressed ubiquitously can exert their effect in a tissue-, cellular compartment-, and isoform-specific manner.

Limb-girdle muscular dystrophies (LGMDs) are a genetically and mechanistically heterogeneous group of disorders caused by dominant or recessive mutations in a number of sarcolemmal, sarcomeric, cytoplasmic, and nuclear proteins[2]. Here we studied the molecular cause of a dominant LGMD in five previously reported Finnish (FF1–5)[3, 4], and two U.S. families (DUK1047 and DUK1701)[1, 5], as well as two new Italian LGMD families (IT1 and IT2) identified on the basis of clinical phenotypes and the pattern of muscle involvement by magnetic resonance imaging. The pedigrees of the studied families are shown in Supplementary Fig. 1, and clinical findings are summarized in Supplementary Table 1.

The disorder in the two U.S. families was linked originally to 7q36 and classified as LGMD1D[1]. Clinical and genetic characterization of the Finnish families then established linkage to the same locus and refined *LGMD1D* to a 3.4-Mb region containing 12 genes[3, 4]. Sequencing of the positional candidates *RNF32, UBE3C, DNAJB6*, and *PTPRN2* revealed a c.279C>G (p.Phe93Leu) change in exon 5 of *DNAJB6* in all 16 affected patients in the Finnish families FF1–5 (nucleotide and protein numberings based on NM_005494.2 and NP_005485.1, respectively). The mutation was absent from 12 unaffected individuals in these families (Table 1, Supplementary Figs. 1, 2). Sequencing of muscle cDNA from two Finnish patients confirmed that the wild-type and mutant alleles were both expressed (Supplementary Fig. 2). Analysis of *DNAJB6* in the two U.S. families revealed a c.267T>A (p.Phe89Ile) mutation in all 29 affected individuals (Table 1), and in two individuals of unknown disease status (below the highest age of onset identified previously in the families). Two discrete *DNAJB6* mutations were identified in the Italian families; c.279C>A (IT1; eight patients) and c.277T>C (IT2; four patients), both leading to the same p.Phe93Leu change as the Finnish mutation (Table 1). Six available healthy individuals in IT1 and four in IT2 had no mutations. None of the mutations were found in 404 Finnish, 208 Italian or 430 U.S. control chromosomes. The presence of multiple independent mutations and their segregation with the phenotype in nine families comprises conclusive genetic evidence that *DNAJB6* is the *LGMD1D* causative gene.

DNAJB6 (also known as MRJ) belongs to the J-proteins (also known as the Hsp40 family), a class of co-chaperones characterized by a J-domain. These co-chaperones interact with the chaperones of the HSPA (Hsp70) family, increasing and modulating their activity (recently reviewed by Kampinga & Craig[6]). Some J-proteins, including DNAJB6, also have HSPA-independent functions[6, 7].

DNAJB6 is composed of a conserved N-terminal J-domain, a G/F-domain rich in glycine and phenylalanine residues, and a C-terminal domain containing a serine-rich (“SSF-SST”) region[7, 8] (Supplementary Fig. 2a). The J-domain interacts with the constitutively expressed chaperone HSPA8 (also known as Hsc70 or Hsp73)[9]. The SSF-SST region has been shown to be important for interactions with NFATc3[10] and HDACs[7], and for DNAJB6 oligomerization[7]. The G/F-domain, harboring the LGMD1D mutations, has been suggested to participate in recognition of partially unfolded client proteins in bacterial DnaJ[11-13] and yeast Sis1[14]. Notably, human DNAJB6 has two known isoforms characterized by alternative

C-termini[15]. The long isoform DNAJB6a (36 kDa) localizes to the nucleus, whereas the short DNAJB6b (27 kDa) is cytoplasmic[15, 16].

DNAJB6 has been reported to suppress aggregation and toxicity of aggregation-prone proteins such as polyglutamine-containing huntingtin and α-synuclein[7, 8, 17], and to participate in autophagic and proteasomal turnover of proteins and organelles[18, 19], as well as in regulation of gene expression[10] and cell cycle[20]. The inhibition of aggregate-induced cytotoxicity may involve myeloid leukemia factor 1 (MLF1), which interacts with DNAJB6 and co-localizes with it in aggregates[21].

DNAJB6 is expressed in all tissues[22] with highest expression in brain[8], but its expression and localization in skeletal muscle has not been characterized previously. Immunofluorescence (IF) microscopy showed DNAJB6 primarily in Z-disks in both control (not shown) and LGMD1D muscle samples (Fig. 1a). Electron microscopy (EM) of LGMD1D patient muscle revealed Z-disk myofibrillar disintegration (Fig. 1b). Autophagic rimmed-vacuolar degenerative pathology was demonstrated by EM (Fig. 1b, Supplementary Fig. 3), LC3 immunohistochemistry, and Herovici staining (Fig. 1c). IF microscopy of patient muscle revealed DNAJB6 in protein accumulations together with its known ligands MLF1[21] and HSPA8[9] (Fig. 1d, Supplementary Fig. 4). Myotilin, desmin, and αB-crystallin, and occasionally filamin—proteins typically aggregating in myofibrillar myopathies—were also observed in these structures. Furthermore, some accumulations stained positive for keratin 18 (KRT18), a reported client protein of DNAJB6[9] (Fig. 1d, Supplementary Fig. 4). Notably, we did not observe accumulation of thick and thin filament components, such as myosins and actin (not shown). For comparison, we examined muscle tissue from a myofibrillar myopathy patient carrying the p.Ser60Cys myotilin mutation, characterized by aggregation of myotilin and other proteins[23]. We found co-localization of DNAJB6, MLF1 and KRT18 with myotilin in these aggregates (Supplementary Fig. 4). In LGMD1D muscle, DNAJB6 appeared more in the periphery of the protein accumulations, in contrast to the more pronounced co-localization seen in myotilinopathy.

To provide further support for the causal involvement of *DNAJB6*, we investigated its roles for muscle integrity *in vivo* in zebrafish. Reciprocal BLAST identified in zebrafish a single *DNAJB6* ortholog (*dnajb6b*). We detected its expression by RT-PCR as early as the embryonic 5-somite stage (data not shown). Next, we injected two-cell stage embryos with a splice-blocking morpholino (sb-MO) targeting *dnajb6b*. Masked scoring of embryos at 48 hours post-fertilization (hpf) showed a reproducible muscle fiber detachment phenotype concomitant with the splice blocking efficiency, as established by RT-PCR (Supplementary Fig. 5a). Detachment of slow fibers from their insertion sites at the vertical myoseptum was evident as early as 2 days post-fertilization (dpf) (Fig. 2), suggesting that the fiber termini in morphants are prone to adhesion failure soon after mechanical load is applied by the onset of strong contraction[24]. The phenotype was specific; it could be reproduced with a second non-overlapping MO (data not shown), and rescued with co-injection of wild-type human *DNAJB6b* mRNA (Fig. 2j). These data suggest that loss of function of DNAJB6 leads to muscle integrity defects.

To understand the mechanistic effect of LGMD1D mutations, we introduced the p.Phe93Leu and p.Phe89Ile changes in human transcripts encoding each of the two isoforms, and injected them in zebrafish embryos. In contrast to wild-type *DNAJB6*, which yielded no appreciable defects, injection of equivalent doses of either p.Phe93Leu or p.Phe89Ile mRNAs phenocopied the loss-of-function effects of the *dnajb6b* sb-MO (Fig. 2). Strikingly, these phenotypes were generated exclusively upon injection of mutant *DNAJB6b*; neither mutation, when engineered into *DNAJB6a*, had any impact (Fig. 2).

All identified LGMD1D mutations map to the G/F-domain of DNAJB6. Both mutated Phe residues are highly conserved in DNAJB6 orthologs, and Phe93 is also conserved in several paralogs (Supplementary Fig. 2). It is unusual that three of the four LGMD1D-causing mutations affect the same codon, leading to the identical p.Phe93Leu change. To determine whether the loss of Phe or the introduction of Leu is more important, we replaced Phe93 with either Ala or Gly. Embryos injected with either p.Phe93Ala or p.Phe93Gly mRNA showed muscle fiber detachment similar to the p.Phe93Leu-induced phenotype (Fig. 2), indicating that the loss of Phe93 is sufficient for the pathogenesis. However, the zebrafish ortholog contains a Gly instead of Phe89, suggesting that some changes might be tolerated in this position; expression of human p.Phe89Gly DNAJB6b in zebrafish embryos did not cause a muscle phenotype (Fig. 2).

Next, we tested whether the *LGMD1D* mutations could be rescued with wild-type DNAJB6. Co-injection of equimolar amounts of p.Phe93Leu and wild-type mRNA into zebrafish embryos showed enhanced severity of the muscular phenotype: in comparison to 15% of embryos injected with mutant *DNAJB6b* alone, 42% of co-injected embryos had severe defects in muscle integrity by 2 dpf (P=0.0004; Fig. 3a). A similar effect was observed with the p.Phe89Ile mutation (P=0.0002; Fig. 3a). Taken together, our data indicate that the phenotype is driven by the dysfunction of the cytoplasmic isoform and suggest that the LGMD-causing mutations likely exert a deleterious dominant effect on the wild-type protein. Consistent with this notion, altering the molar ratios of mutant and wild-type mRNA had the expected effects on the phenotype. An excess of mutant to wild-type mRNA induced lethality in embryos, while an excess of wild-type to mutant mRNA gave rise to progressively increased rescue (Supplementary Fig. 5c).

We next turned to *in vitro* experiments. Based on evidence from the closely related DNAJB8 protein, DNAJB6 has been suggested to form oligomeric complexes[7]. As interfering with the complex formation could explain the dominant effect of the mutations, we studied the oligomerization of wild-type and p.Phe93Leu DNAJB6b in COS-1 cells. In coimmunoprecipitation (CoIP) experiments, V5-tagged DNAJB6b pulled down the untagged construct, demonstrating oligomerization (Supplementary Fig. 6a), and this was unaffected by the p.Phe93Leu mutation. Likewise, in sucrose density gradient centrifugation, the distribution of wild-type and mutant constructs was similar (Supplementary Fig. 6b). Hence, the p.Phe93Leu mutation did not significantly alter the oligomerization properties of DNAJB6.

We next turned to the possibility that *LGMD1D* mutations might alter DNAJB6 half-life, as we observed that cells transfected with DNAJB6b showed an increase in mutant protein

abundance with no appreciable changes in mRNA levels (data not shown). To examine this, we transfected 293FT cells, followed by blocking protein synthesis with cycloheximide (CHX) and quantifying the amounts of remaining protein as a function of time (Fig. 3b, Supplementary Fig. 7). Both p.Phe93Leu and p.Phe89Ile decreased significantly the turnover rate of DNAJB6. To explore whether the increased abundance of mutant DNAJB6 might be proteasome or autophagosome-dependent, we treated DNAJB6-transfected cells either with a proteasome poison (lactacystin) or a lysosome inhibitor (bafilomycin A1). Suppression of the proteasome had no appreciable effects on the clearance of DNAJB6. By contrast, the bafilomycin treatment (in the presence of CHX) led to a significant (40–50%) increase of DNAJB6, suggesting that, at least in part, DNAJB6 is cleared by the autophagosome pathway (Supplementary Fig. 7). This is also consistent with the observation that DNAJB6 abundance was reduced in the presence of both lactacystin and CHX (compared to CHX alone), since suppression of the proteasome has been reported to enhance autophagy[25-27].

The ability of mutant DNAJB6 to oligomerize, the observed increased abundance of mutant protein, and the exacerbation of the zebrafish phenotypes by co-injection of wild-type mRNA suggested that mutant DNAJB6 might affect the entire oligomeric complex. To assay this, we co-transfected cells with mutant and wild-type DNAJB6b. Not only did the mutant protein decrease the turnover of the wild-type protein, but the stability of the mutant itself increased further in the presence of wild-type DNAJB6 (Fig. 3b). These data confirm that mutant DNAJB6 can exert a dominant effect on the wild-type protein.

A possible explanation for the increased abundance of mutant/wild-type protein complexes would be formation of aggregates. However, we did not detect any increased aggregation propensity of the mutants in cell fractionation, sucrose density gradient centrifugation, or IF microscopy of transfected cells (not shown). Hence, primary aggregation of DNAJB6 is unlikely to underlie the pathogenesis of LGMD1D. This is in line with the muscle pathology revealing DNAJB6 in the periphery, rather than in the center, of the protein accumulations.

DNAJB6 has been shown to suppress aggregation of various proteins in cell culture models[7, 8, 28]. To investigate the effect of the mutations on the anti-aggregation function, we tested the ability of wild-type and mutant DNAJB6b to inhibit aggregation of polyglutamine-containing huntingtin (pEGFP/HD-120Q) in a filter trap assay (FTA). The nuclear DNAJB6a isoform, known to be inefficient towards cytoplasmic huntingtin aggregation[7], served as negative control. In line with Hageman *et al.*[7], wild-type DNAJB6b efficiently suppressed huntingtin aggregation, as demonstrated by a decrease in the aggregate amount and a concomitant increase in SDS-soluble huntingtin (Fig. 4, Supplementary Fig. 8). In contrast, mutant constructs showed significantly impaired anti-aggregation function, although they still retained some activity. This compromised function could impair protein quality control in LGMD1D muscle, ultimately leading to protein accumulation.

Chaperone-assisted selective autophagy (CASA), mediated by a complex containing HSPA8, BAG3, STUB1 (also known as CHIP), and HSPB8 (also known as Hsp22), is important for Z-disk maintenance[29, 30]. Several pieces of evidence prompted us to

investigate the link between DNAJB6 and CASA. First, DNAJB6 is a known co-chaperone of HSPA8[8]. Second, the pathology of LGMD1D muscle suggests defective Z-disk maintenance. Third, both DNAJB6 and the CASA complex localize to the Z-disk. Finally, mutations in BAG3 cause a myofibrillar myopathy with protein accumulations and autophagic pathology[31]. To study the possible association of DNAJB6 with the CASA complex, we performed CoIP studies of endogenous and transfected proteins in COS-1 cells, and observed interaction of DNAJB6b with BAG3, HSPB8, and STUB1 (Fig. 5a, Supplementary Fig. 9). Association of DNAJB6 with the CASA machinery was also supported by *in situ* proximity ligation assay (PLA) studies on rat muscles (Fig. 5b). None of the interactions seemed to be affected by the p.Phe93Leu mutation (Fig. 5a, Supplementary Fig. 9), indicating that the phenotype is unlikely to be caused by impaired binding of DNAJB6 to the CASA complex.

The interaction with DNAJB6 suggested a possible role for BAG3 in LGMD1D and implied a pathomechanistic link between LGMD1D and the BAG3 myopathy. We therefore asked whether BAG3 could modulate the phenotype caused by mutant DNAJB6b in zebrafish. Surprisingly, while injection of wild-type BAG3 alone caused no observable phenotype, its co-injection with DNAJB6b p.Phe93Leu accentuated dramatically the muscle defect caused by the mutation (P=0.02; Fig. 5c). In addition, while injection of the BAG3 myopathy mutant (p.Pro209Leu)[31] alone led to a phenotype comparable to DNAJB6 mutants, its co-injection with DNAJB6b p.Phe93Leu did not have an additive effect. These findings strongly suggest that BAG3 plays an active role in mediating the dominant pathogenic effect of DNAJB6b mutations and that it likely lies downstream of DNAJB6.

We have described here the first human mutations in the ubiquitously expressed, multifunctional co-chaperone DNAJB6. This protein has been implicated previously in a variety of degenerative disorders such as Parkinson's[17] and Huntington's[8] diseases, as well as cancer[16]. Surprisingly, the identified *DNAJB6* mutations cause a tissue- and isoform-specific disease, muscular dystrophy; despite the high expression of DNAJB6 in the brain, there are no indications of neurological involvement[3-5].

The four LGMD1D mutations all affect two highly conserved, closely spaced phenylalanine residues in the G/F-domain. The mutations impair the anti-aggregation activity of DNAJB6b and interfere with the turnover of both mutant and wild-type DNAJB6b. The unexpected finding that addition of wild-type DNAJB6b exacerbates the muscular phenotype induced by each mutation in zebrafish suggests that incorporation of mutant protein to the DNAJB6 oligomer likely confers a dominant toxic function to the entire complex. Moreover, the interaction of BAG3 with DNAJB6, and its aggravating effect on the zebrafish phenotype suggest a direct role for BAG3 in the pathomechanism. The myofibrillar disintegration with protein accumulations in LGMD1D muscle could therefore reflect impaired function of the CASA machinery, leading to insufficient maintenance of sarcomeric structures or defective clearance of misfolded sarcomeric proteins.

The *DNAJB6* mutations cause a dominant late onset muscle disease characterized by abnormal protein accumulations and autophagic pathology. Although the mutations are expressed in both nuclear and cytoplasmic DNAJB6, they affect muscle pathology

exclusively through the cytoplasmic isoform. This is reminiscent of the mechanism proposed for Lafora progressive myoclonus epilepsy, in which mutations in *EPM2A* are expressed in both the nucleus and the cytoplasm, but appear to interfere specifically with its cytoplasmic phosphatase activity[32]. Surprisingly, the literature is largely bereft of other such examples, despite the documented prevalence of alternative splicing[33]. Elucidation of the mechanisms by which certain isoforms of mutated ubiquitously expressed proteins can lead to organ-specific effects will be important for understanding genetic diseases and for the development of therapeutical options.

Methods

Patients and muscle biopsies

The Finnish families FF1–FF5, and U.S. families, DUK1047, and DUK1701 have been described previously[1, 3-5]. Biopsy materials were primarily obtained from the Finnish families. Previous diagnostic muscle biopsies from the DUK families were reviewed. All examinations were performed with informed consent according to the Helsinki declaration. Studies were approved by local ethical committees.

Sequencing

PCR reactions and Sanger sequencing were performed with standard methods. Sequences were analyzed with Sequencher 4.8 (Genes Codes Corporation, Ann Arbor, MI, USA).

RNA isolation and RT-PCR

RNA was isolated from muscle biopsies using the Dr.P kit (BioChain Institute, Inc., Hayward, CA, USA) and reverse transcribed using SuperScript II (Invitrogen Co., Carlsbad, CA, USA). Target sequences were amplified with DreamTaq (Fermentas GmbH, St. Leon-Rot, Germany) and sequenced.

Primary antibodies

Commercial primary antibodies were from Abcam plc, Cambridge, UK (HSPA8, HSPB8, KRT18, MLF1, α-tubulin); Abnova, Taipei, Taiwan (DNAJB6); Calbiochem, Merck Chemicals, Darmstadt, Germany (STUB1); Cell Signaling Technology, Danvers, MA, USA (HSPB8); DSHB, Iowa City, IA, USA (myosin heavy chain); Epitomics, Inc., Burlingame, CA, USA (desmin); Invitrogen (V5); Novocastra, Leica Microsystems GmbH, Wetzlar, Germany (αB-crystallin); Novus Biologicals, Inc., Littleton, CO, USA (LC3); Proteintech Group, Inc., Chicago, IL, USA (BAG3); Sigma-Aldrich, St. Louis, MO, USA (filamin, GFP, HA, α-tubulin); Santa Cruz Biotechnology, Inc, Santa Cruz, CA, USA (GFP, HSP90). Myotilin antibody[34] was a gift from Olli Carpén. For details, see Supplementary Table 2.

Electron microscopy

Muscle specimens were fixed in 2% glutaraldehyde in 0.1 M phosphate buffer o/n at 4°C, washed in 0.1 M phosphate buffer, dehydrated, embedded in Epon blocks, sectioned, and imaged by transmission electron microscopy.

Immunofluorescence stainings and microscopy

Muscles were embedded in Tissue-Tek O.C.T. medium (Sakura Finetek Europe B.V., Zoeterwoude, The Netherlands), frozen in liquid-nitrogen-chilled isopentane, and sectioned. For IF, the sections were fixed with 4% PFA in PBS 10 min RT, permeabilized with 0.2% Triton X-100 in PBS 10 min, blocked with 5% BSA in PBS 30 min, and immunostained with antibodies in 1% BSA in PBS. Immunohistochemical and histological stainings were performed according to standard procedures. For wholemount IF, zebrafish embryos were fixed in 4% PFA o/n and stored in 100% methanol at −20°C. After rehydratation in PBS, embryos were washed in 0.1% Tween-20, 1% BSA in PBS 10 min RT, incubated in blocking buffer (10% FBS, 1% BSA in PBS) 1 h RT, and immunostained with antibodies in blocking buffer. Primary antibody incubations were 1–2 h RT (sections) or o/n at 4–8°C (zebrafish embryos). Alexa Fluor -labeled secondary antibodies were from Molecular Probes, Invitrogen.

Widefield fluorescence microscopy was performed using Zeiss Axioplan 2 (Carl Zeiss MicroImaging GmbH, Göttingen, Germany) or AZ100 (Nikon Instruments Inc., Melville, NY, USA). Confocal microscopy was performed using LSM 510 Meta (Carl Zeiss MicroImaging) with a 63×/NA 1.4 objective. Image processing and analysis were done using the LSM 510 Meta 3.2 software (Carl Zeiss MicroImaging), Adobe Photoshop CS4 11.0.2 (Adobe Systems Inc., San Jose, CA, USA), and ImageJ 1.41o (Rasband W.S., NIH, Bethesda, MD, USA; http://rsb.info.nih.gov/ij/).

SDS-PAGE and western blotting

SDS-PAGE and WB were performed according to standard methods. Blots were visualized with chemiluminescence using film or a ChemiDoc XRS+ system (Bio-Rad Laboratories, Hercules, CA, USA), or fluorescent detection with the Odyssey system (LI-COR Biosciences, Lincoln, NE, USA).

Plasmid constructs

Coding regions of human *DNAJB6a* and *DNAJB6b* were cloned into pEF6/V5-His TOPO (Invitrogen) (in frame with the C-terminal V5/His_6 tag or including the native stop codon), pCS2, pCMV-HA (Clontech Laboratories, Inc., Mountain View, CA, USA), and into a Gateway GFP vector. To generate the inducible DNAJB6-V5 constructs, inserts including the tag were transferred from the pEF6 constructs into pcDNA5/TO (Invitrogen). Coding region of human *BAG3* was cloned into a Gateway version of pCS2. The desired mutations were introduced to DNAJB6 and BAG3 by site-directed mutagenesis. The huntingtin construct pEGFP/HD-120Q[35], STUB1 construct in pcDNA3.1/Myc-His[36], and titin construct is6–M9-V5[37] have been described.

Zebrafish studies

Zebrafish (*Danio rerio*) embryos were raised and fish were maintained as described[38]. Embryos at 24 h post-fertilization (hpf) were raised in 0.2 mM 1-phenyl-2-thio-urea (Sigma-Aldrich) to prevent pigment formation and allowed to develop until 48 hpf. Embryos at 1- or 2-cell stage were injected with the *dnajb6b* splice-blocking morpholino oligonucleotide

(AAATATCCAATACCATCTGACAGGA, dose of 6 ng), or with capped mRNA (50 pg per injection unless otherwise specified) transcribed *in vitro* from the pCS2 constructs using the Ambion mMessage mMachine SP6 Kit (Invitrogen). Embryos were scored at 48 hpf for relative muscular defects, compared with age-matched controls from the same clutch.

Cell cultures and transfections

COS-1 (ATCC), 293FT (Invitrogen), and T-REx 293 (Invitrogen) were cultured at 37°C, 5% CO_2 in DMEM with 10% FCS and L-glutamine. Media were supplemented with penicillin/streptomycin (for COS-1 and T-REx 293), and 5 μg/ml blasticidin S (for T-REx 293). Transfections were done with FuGENE 6 (Roche Applied Science, Basel, Switzerland).

Turnover assays and drug treatments

293FT cells were transfected at 70% confluency with wt or mutant HA- or GFP-tagged DNAJB6. 48 h post-transfection, the medium was replaced with fresh medium containing 50 μg/ml cycloheximide (Sigma-Aldrich), and optionally 20 μM lactacystin (EMD Chemicals Inc., Gibbstown, NJ, USA) or 100 nM bafilomycin A1 (Sigma-Aldrich). At indicated time points, cells were washed twice with PBS and lysed with RIPA supplemented with Complete Protease Inhibitor Cocktail (Complete; Roche Applied Science). Lysates were centrifuged 10 min at 15,800 × *g*, 4°C, and supernatants analyzed by western blotting. Bands were quantified with Quantity One (Bio-Rad). The ratios of DNAJB6 constructs to α-tubulin or HSP90 were plotted against time. For time-series experiments, the ratio at $t = 0$ h was set to 100% for each construct.

Coimmunoprecipitation (CoIP)

COS-1 were collected 1–2 days post-transfection, lysed with ice-cold 10 mM Tris-HCl pH 7.5, 10 mM NaCl, 2 mM EDTA, 0.5% Triton X-100, 1× Complete, and incubated on ice 10 min. NaCl was added to 150 mM. The lysates were incubated on ice 5 min, and centrifuged 15 min at 16,000 × *g*, 8°C. After removing total protein samples, the lysates were rotated with anti-V5 beads (Novus Biologicals) o/n at 8°C. The beads were washed 4–6 times with ice-cold 50 mM Tris-HCl pH 7.5, 150 mM NaCl, 0.05% Triton X-100.

Alternatively, for experiments with crosslinking, cells were lysed in ice-cold PBS containing 0.5% Triton X-100, 1× Complete, by triturating through a 27G needle, and centrifuged 15 min at 16,000 × *g*, 8°C. The lysates were crosslinked with 1 mM dithiobis[succinimidyl propionate] (Pierce, Thermo Fisher) (from 20 mM stock in DMSO) 30 min on ice. Crosslinking was stopped with 20 mM Tris-HCl pH 7.4, 15 min on ice. After removing total protein samples, the lysates were rotated with anti-V5 beads 2–4 h at 8°C. The beads were washed three times with ice-cold RIPA (50 mM Tris-HCl pH 7.5, 150 mM NaCl, 1% NP-40, 0.5% Na-deoxycholate, 0.1% SDS).

Bound proteins were eluted into 2× SDS sample buffer with 10% 2-mercaptoethanol 95°C, 5 min.

Density gradient centrifugation

Density gradient centrifugation protocol was adapted from Hageman *et al*.[7]. COS-1 cells were transfected with pEF6-DNAJB6b wild-type or p.Phe93Leu. After 24h, cells were lysed with 10 mM Tris-HCl pH 8.0, 150 mM NaCl, 0.5% NP-40, 3% glycerol, 1× Complete, and centrifuged 15 min at 300 × *g*. Supernatants were loaded on 10–80% sucrose gradients in 10 mM Tris-HCl pH 8.0, 50 mM NaCl, 5 mM EDTA, and centrifuged for 18–20 h at 100,000 × *g*, 8°C. The gradients were fractionated and proteins precipitated with TCA essentially as described[7].

Filter trap assay (FTA)

T-REx 293 cells, plated on collagen-coated 6-well plates at 150,000 cells/well, were cotransfected with 875 ng of pcDNA5/TO-DNAJB6 and 125 ng of pEGFP/HD-120Q. Each transfection was done in duplicate, and after 7 h DNAJB6 expression was induced in one of the duplicates with 1 μg/ml tetracycline. 48 h post-transfection, FTA was performed according to a protocol adapted from Hageman *et al*.[7]: The cells were lysed with 750 μl of FTA buffer (10 mM Tris-HCl pH 8.0, 150 mM NaCl, 50 mM dithiothreitol) containing 2% SDS and 1× Complete, triturated through a 27G needle, sonicated 1 min in bath, and heated to 98°C. Samples for SDS-PAGE analysis of soluble huntingtin were removed, and 100–150 μl of the remaining lysates were filtered through a cellulose acetate membrane (pore size 0.2 μm, Whatman GmbH, Dassel, Germany), followed by three washes with 300 μl FTA buffer containing 0.1% SDS.

FTA membranes and western blots of SDS-soluble huntingtin were immunostained with GFP antibody, visualized using fluorescent detection, and quantified with the Odyssey software (LI-COR). Aggregation scores ($[\text{aggr./sol}]_{\text{induced}}/[\text{aggr./sol.}]_{\text{uninduced}}$) were calculated from the amounts of aggregated (aggr.) and soluble (sol.) huntingtin in the uninduced and induced cells in each transfection pair. Each construct was tested in three experiments performed in quadruplicate.

In situ proximity ligation assay (PLA)

PLA was done on rat *gastrocnemius* muscle sections using the Duolink kit (Olink Bioscience, Uppsala, Sweden). The samples were prepared and PLA performed essentially as described previously[37].

Statistical analysis

Results were analyzed with two-tailed Mann-Whitney *U* test with Bonferroni correction (filter trap assay), or with the χ^2 test (zebrafish phenotype distributions).

Supplementary Material

Refer to Web version on PubMed Central for supplementary material.

Acknowledgments

This study was supported by the Folkhälsan Research Foundation (504; B.U.), the Academy of Finland (138491; B.U.), the Sigrid Jusélius Foundation (23816; B.U.), the Liv och Hälsa Foundation (LoH G017; B.U.), Helsinki

Graduate School in Biotechnology and Molecular Biology (J.S.), the Alfred Kordelin Foundation (J.S.), the Don Carlo Gnocchi Onlus Foundation (RF 2007 convenzione 41; G.T, E.R.), the American Heart Association (AHA MAA spring 2011 #11POST7160006; C.G.), the Duke Perinatal and Neonatal Research Institute (N.K.), the National Institutes of Health (UL 1RR024128; N.K., M.H., and 5R01-042601-09; C.G.), and the Muscular Dystrophy Association (MDA4090, MDA2010; M.H.). N.K. is a Distinguished Brumley Professor.

We thank Olli Carpén (Dept. of Pathology, University of Helsinki) for the myotilin antibody; Anne Nørremølle (Faculty of Health Sciences, University of Copenhagen) for the pEGFP/HD-120Q construct; Cam Patterson (School of Medicine, University of North Carolina) for the STUB1 construct; Mirkka Sarparanta (Lab. of Radiochemistry, University of Helsinki) for rat muscles; and Merja Soininen, Marjut Ritala, and Anni Evilä for technical assistance.

Confocal microscopy was carried out with instruments of the Biomedicum Imaging Unit, and electron microscopy at the Dept. of Pathology, University of Helsinki.

References

1. Speer MC, et al. Identification of a new autosomal dominant limb-girdle muscular dystrophy locus on chromosome 7. Am J Hum Genet. 1999; 64:556–562. [PubMed: 9973293]
2. Gordon, E.; Pegoraro, E.; Hoffman, EP. Gene Reviews. Pagon, RA.; Bird, TD.; Dolan, CR.; Stephens, K., editors. University of Washington, Seattle; Seattle (WA): 1993.
3. Sandell S, et al. The enigma of 7q36 linked autosomal dominant limb girdle muscular dystrophy. J Neurol Neurosurg Psychiatry. 2010; 81:834–839. [PubMed: 20682716]
4. Hackman P, et al. Four new Finnish families with LGMD1D; refinement of the clinical phenotype and the linked 7q36 locus. Neuromuscul Disord. 2011; 21:338–344. [PubMed: 21376592]
5. Speer MC, et al. Evidence for locus heterogeneity in autosomal dominant limb-girdle muscular dystrophy. Am J Hum Genet. 1995; 57:1371–1376. [PubMed: 8533766]
6. Kampinga HH, Craig EA. The HSP70 chaperone machinery: J proteins as drivers of functional specificity. Nat Rev Mol Cell Biol. 2010; 11:579–592. [PubMed: 20651708]
7. Hageman J, et al. A DNAJB chaperone subfamily with HDAC-dependent activities suppresses toxic protein aggregation. Mol Cell. 2010; 37:355–369. [PubMed: 20159555]
8. Chuang JZ, et al. Characterization of a brain-enriched chaperone, MRJ, that inhibits Huntingtin aggregation and toxicity independently. J Biol Chem. 2002; 277:19831–19838. [PubMed: 11896048]
9. Izawa I, et al. Identification of Mrj, a DnaJ/Hsp40 family protein, as a keratin 8/18 filament regulatory protein. J Biol Chem. 2000; 275:34521–34527. [PubMed: 10954706]
10. Dai YS, Xu J, Molkentin JD. The DnaJ-related factor Mrj interacts with nuclear factor of activated T cells c3 and mediates transcriptional repression through class II histone deacetylase recruitment. Mol Cell Biol. 2005; 25:9936–9948. [PubMed: 16260608]
11. Perales-Calvo J, Muga A, Moro F. Role of DnaJ G/F-rich domain in conformational recognition and binding of protein substrates. J Biol Chem. 2010; 285:34231–34239. [PubMed: 20729526]
12. Cajo GC, et al. The role of the DIF motif of the DnaJ (Hsp40) co-chaperone in the regulation of the DnaK (Hsp70) chaperone cycle. J Biol Chem. 2006; 281:12436–12444. [PubMed: 16533811]
13. Wall D, Zylicz M, Georgopoulos C. The conserved G/F motif of the DnaJ chaperone is necessary for the activation of the substrate binding properties of the DnaK chaperone. J Biol Chem. 1995; 270:2139–2144. [PubMed: 7836443]
14. Yan W, Craig EA. The glycine-phenylalanine-rich region determines the specificity of the yeast Hsp40 Sis1. Mol Cell Biol. 1999; 19:7751–7758. [PubMed: 10523664]
15. Hanai R, Mashima K. Characterization of two isoforms of a human DnaJ homologue, HSJ2. Mol Biol Rep. 2003; 30:149–153. [PubMed: 12974469]
16. Mitra A, et al. Large isoform of MRJ (DNAJB6) reduces malignant activity of breast cancer. Breast Cancer Res. 2008; 10:R22. [PubMed: 18328103]
17. Durrenberger PF, et al. DnaJB6 is present in the core of Lewy bodies and is highly up-regulated in parkinsonian astrocytes. J Neurosci Res. 2009; 87:238–245. [PubMed: 18711724]
18. Watson ED, Geary-Joo C, Hughes M, Cross JC. The Mrj co-chaperone mediates keratin turnover and prevents the formation of toxic inclusion bodies in trophoblast cells of the placenta. Development. 2007; 134:1809–1817. [PubMed: 17409114]

19. Rose JM, Novoselov SS, Robinson PA, Cheetham ME. Molecular chaperone-mediated rescue of mitophagy by a Parkin RING1 domain mutant. Hum Mol Genet. 2011; 20:16–27. [PubMed: 20889486]
20. Zhang Y, et al. The Hsp40 family chaperone protein DnaJB6 enhances Schlafen1 nuclear localization which is critical for promotion of cell-cycle arrest in T-cells. Biochem J. 2008; 413:239–250. [PubMed: 18373498]
21. Li ZF, et al. Non-pathogenic protein aggregates in skeletal muscle in MLF1 transgenic mice. J Neurol Sci. 2008; 264:77–86. [PubMed: 17854834]
22. Seki N, et al. Cloning, tissue expression, and chromosomal assignment of human MRJ gene for a member of the DNAJ protein family. J Hum Genet. 1999; 44:185–189. [PubMed: 10319584]
23. Selcen D, Engel AG. Mutations in myotilin cause myofibrillar myopathy. Neurology. 2004; 62:1363–1371. [PubMed: 15111675]
24. Kimmel CB, Ballard WW, Kimmel SR, Ullmann B, Schilling TF. Stages of embryonic development of the zebrafish. Dev Dyn. 1995; 203:253–310. [PubMed: 8589427]
25. Ding WX, et al. Linking of autophagy to ubiquitin-proteasome system is important for the regulation of endoplasmic reticulum stress and cell viability. Am J Pathol. 2007; 171:513–524. [PubMed: 17620365]
26. Pandey UB, et al. HDAC6 rescues neurodegeneration and provides an essential link between autophagy and the UPS. Nature. 2007; 447:859–863. [PubMed: 17568747]
27. Zhu K, Dunner K Jr, McConkey DJ. Proteasome inhibitors activate autophagy as a cytoprotective response in human prostate cancer cells. Oncogene. 2010; 29:451–462. [PubMed: 19881538]
28. Hageman J, van Waarde-Verhagen M, Zylicz A, Walerych D, Kampinga HH. The diverse members of the mammalian HSP70 machine show distinct chaperone-like activities. Biochem J. 2011; 435:127–142. [PubMed: 21231916]
29. Arndt V, et al. Chaperone-assisted selective autophagy is essential for muscle maintenance. Curr Biol. 2010; 20:143–148. [PubMed: 20060297]
30. Kettern N, Dreiseidler M, Tawo R, Höhfeld J. Chaperone-assisted degradation: multiple paths to destruction. Biol Chem. 2010; 391:481–489. [PubMed: 20302520]
31. Selcen D, et al. Mutation in BAG3 causes severe dominant childhood muscular dystrophy. Ann Neurol. 2009; 65:83–89. [PubMed: 19085932]
32. Ianzano L, et al. Loss of function of the cytoplasmic isoform of the protein laforin (EPM2A) causes Lafora progressive myoclonus epilepsy. Hum Mutat. 2004; 23:170–176. [PubMed: 14722920]
33. Wang ET, et al. Alternative isoform regulation in human tissue transcriptomes. Nature. 2008; 456:470–476. [PubMed: 18978772]
34. Mologni L, Moza M, Lalowski MM, Carpén O. Characterization of mouse myotilin and its promoter. Biochem Biophys Res Commun. 2005; 329:1001–1009. [PubMed: 15752755]
35. Hasholt L, et al. Antisense downregulation of mutant huntingtin in a cell model. J Gene Med. 2003; 5:528–538. [PubMed: 12797118]
36. Qian SB, McDonough H, Boellmann F, Cyr DM, Patterson C. CHIP-mediated stress recovery by sequential ubiquitination of substrates and Hsp70. Nature. 2006; 440:551–555. [PubMed: 16554822]
37. Sarparanta J, et al. Interactions with M-band titin and calpain 3 link myospryn (CMYA5) to tibial and limb-girdle muscular dystrophies. J Biol Chem. 2010; 285:30304–30315. [PubMed: 20634290]
38. Westerfield, M. The Zebrafish Book. A Guide for the Laboratory Use of Zebrafish (Danio rerio). University of Oregon Press; Eugene, OR: 1995.

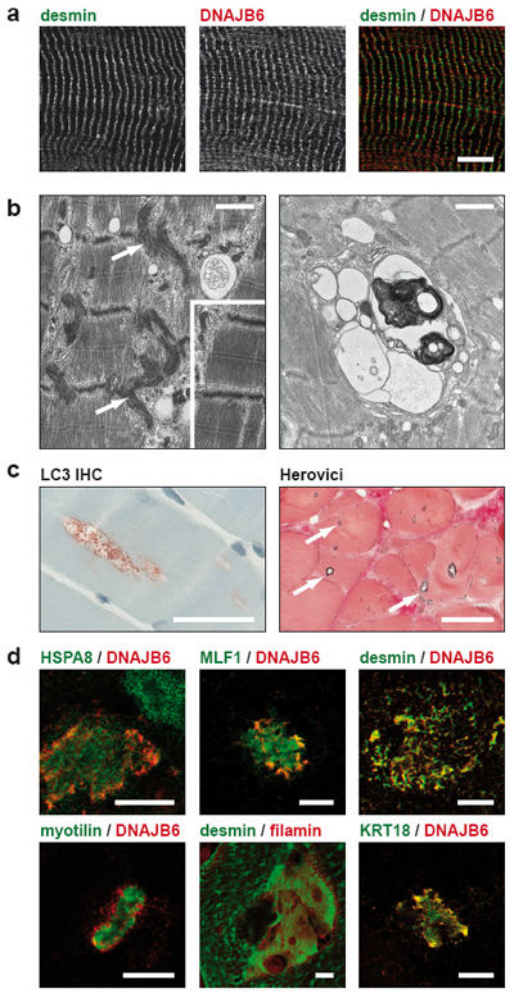

Figure 1.

Microscopy of muscle biopsies from Finnish LGMD1D patients. (**a**) Confocal microscopy of LGMD1D muscle showed that the predominant localization of DNAJB6 in the Z-disc was preserved in the regions with unaltered sarcomeric structure. Scale bar, 10 μm. (**b**) Transmission electron microscopy showed early disruption of Z-disks (arrows; left panel) and authophagic pathology (right panel) in LGMD1D. For comparison, see region with normal ultrastructure (boxed in left panel). Scale bars, approx. 1 μm. (**c**) The autophagic pathology was highlighted by areas of LC3 accumulation within myofibers, revealed by brown precipitate in LC3 immunohistochemistry (left panel), and by the presence of rimmed vacuoles in the Herovici staining (arrows; right panel). Scale bars, approx. 50 μm. (**d**) DNAJB6, HSPA8, MLF1, desmin, myotilin, filamin, and KRT18 were found in protein accumulations. For individual channels, see Supplementary Fig. 4. Confocal images show single optical sections. Scale bars, 10 μm.

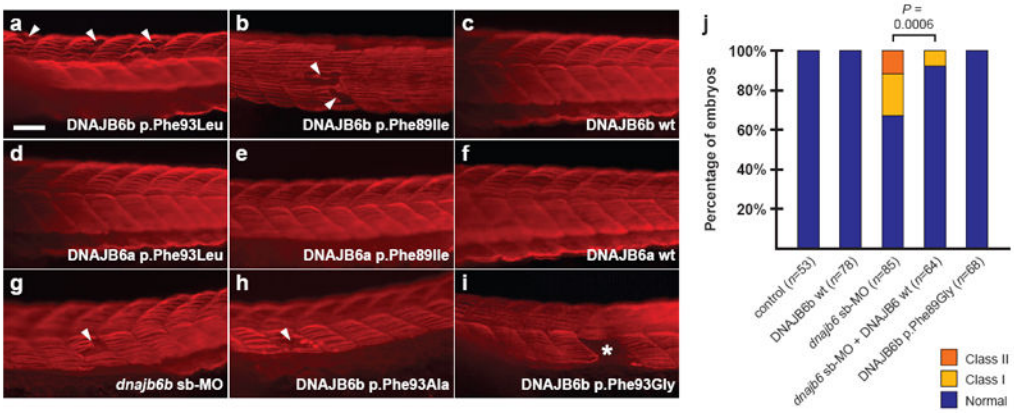

Figure 2.

Muscle disintegration in *DNAJB6b* mutant and morphant zebrafish. (**a–i**) Lateral views of fish embryos 2 dpf subjected to whole-mount immunofluorescence staining of slow myosin heavy chain. Injected embryos expressing wild-type (wt) DNAJB6a/b showed slow myofibers spanning the somite normally between adjacent myosepta (**c, f**) and were indistinguishable from control embryos. Injection of *DNAJB6b* p.Phe93Leu and p.Phe89Ile mutant mRNAs resulted in detachment of fibers from the vertical myoseptum (**a, b**), whereas *DNAJB6a* mutants appeared normal (**d, e**). Similar muscular disintegration was observed in *dnajb6b* morphant embryos injected with sb-MO against the zebrafish ortholog of *DNAJB6* (**g**) and in embryos expressing DNAJB6 p.Phe93Ala or p.Phe93Gly (**h, i**). The detachment of myofibers from the myoseptum can be partial (**a, b, g, h**, white arrowheads) or complete (**i**, white asterisk). Scale bar, approx. 50 μm. (**j**) Embryos injected with the indicated constructs were categorized phenotypically based on the presence of muscle fiber detachment affecting 1–2 somites (class I, mild) or multiple somites (class II, severe; see Supplementary Fig. 5 for an example). The phenotype in *dnajb6b* MO-injected embryos was rescued efficiently by wild-type human *DNAJB6b* mRNA (χ^2 test).

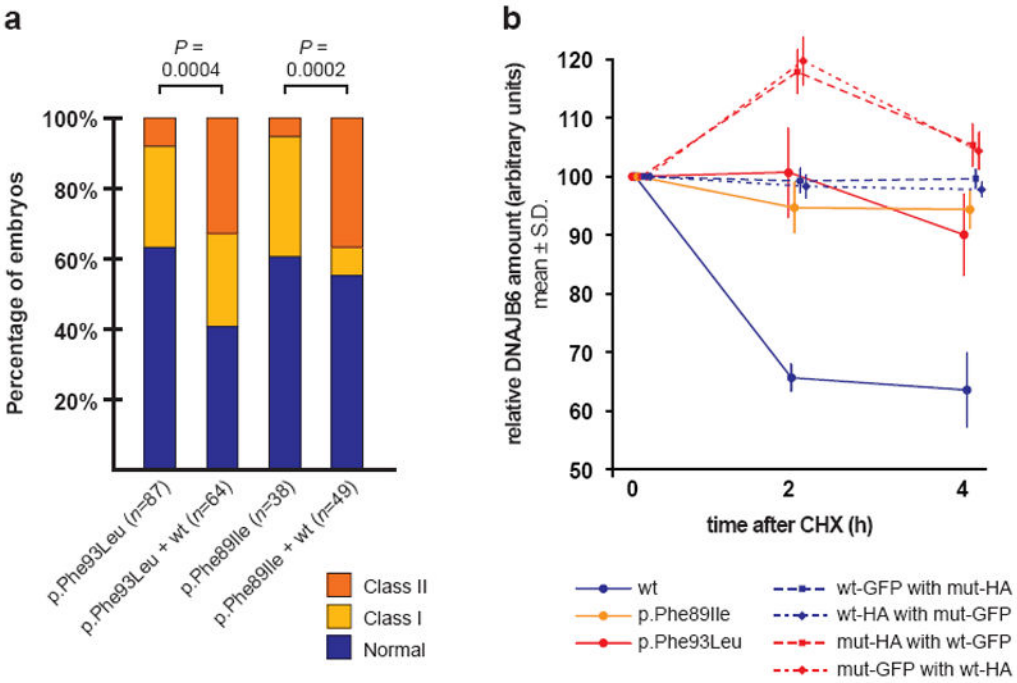

Figure 3.

Dominant effect of mutant DNAJB6 proteins. (**a**) Co-injection of wild-type *DNAJB6b* mRNA with p.Phe93Leu or p.Phe89Ile mutant mRNA in zebrafish embryos led to a more severe muscle phenotype, with a statistically significant increase in the number of class II embryos (χ^2 test). (**b**) *DNAJB6b* constructs were expressed in 293FT cells and protein synthesis was blocked by cycloheximide (CHX). Whole-cell extracts were obtained at the indicated time points and analyzed by western blotting. DNAJB6 band intensities were quantified and normalized to α-tubulin (single transfections) or HSP90 (co-transfections) intensity to obtain the relative DNAJB6 levels. In single transfections (solid lines), cycloheximide treatment rapidly decreased wild-type DNAJB6b protein levels, while p.Phe89Ile and p.Phe93Leu mutant proteins showed reduced turnover. In co-transfections with p.Phe93Leu (dashed lines), the wild-type DNAJB6b level remained stable after 4 h of CHX treatment. Data from three independent experiments are presented as mean ± S.D. Relative DNAJB6 level at t = 0 h was set to 100 for each construct. Representative western blots are shown in Supplementary Fig. 7.

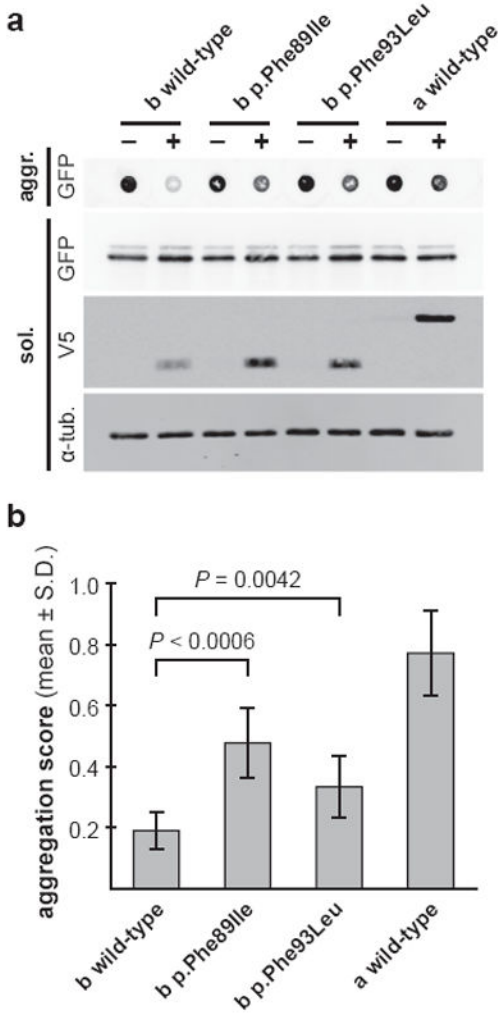

Figure 4.

Impaired anti-aggregation activity of mutant DNAJB6b. GFP-tagged 120Q-huntingtin was expressed in T-REx 293 cells, with co-expression of V5-tagged wild-type or mutant (p.Phe89Ile, p.Phe93Leu) DNAJB6b, or wild-type DNAJB6a induced (+) or uninduced (−). (**a**) Aggregated huntingtin (aggr.) was detected in a filter trap assay, while SDS-soluble huntingtin (sol.), DNAJB6 (V5), and α-tubulin (α-tub.) were analyzed by western blotting. FTA and WB show representative samples. (**b**) Aggregated and soluble huntingtin were quantified, and anti-aggregation activity of DNAJB6 constructs was determined as the ratio of aggr./sol. ratios in induced vs. uninduced cells (aggregation score). Both mutant DNAJB6b constructs showed significantly impaired anti-aggregation activity (Mann-Whitney *U* test; *P* values adjusted for multiple testing with the Bonferroni correction). The nuclear DNAJB6a construct, used as a negative control, showed only weak activity. For each construct, $n = 12$ (3 experiments performed in quadruplicate). For supporting information, see Supplementary Fig. 8.

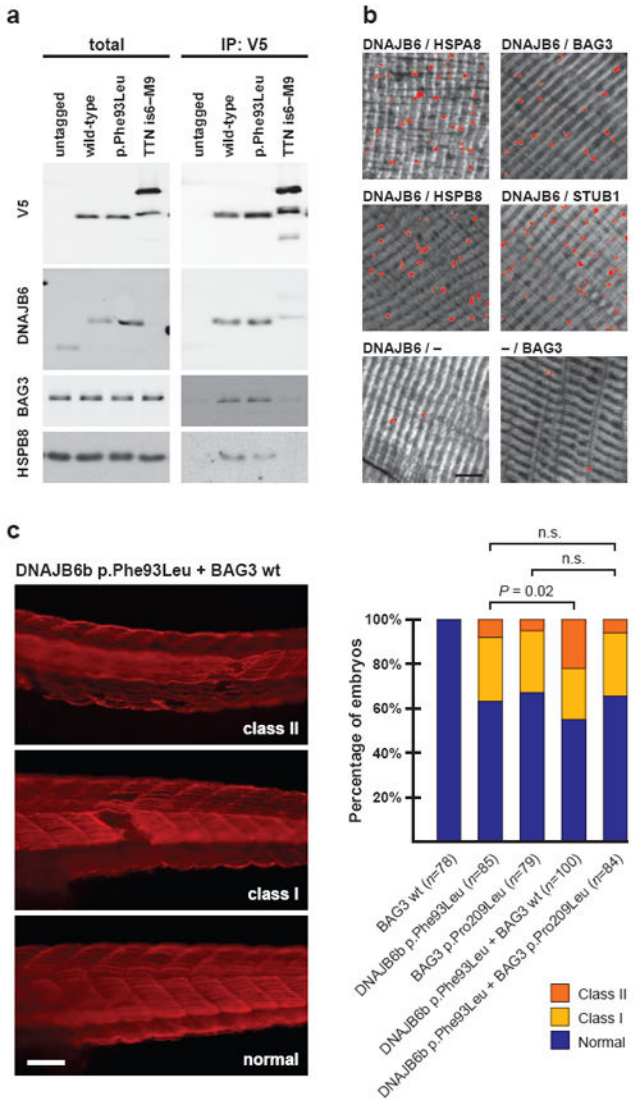

Figure 5.

Association of DNAJB6 with the CASA complex. (**a**) Coimmunoprecipitation. Tested constructs were expressed in COS-1 cells, crosslinked, and immunoprecipitated with anti-V5 beads. V5-tagged wild-type and p.Phe93Leu mutant DNAJB6b pulled down endogenous BAG3 and HSPB8. No coimmunoprecipitation was observed with an untagged DNAJB6b construct or a non-related bait (V5-tagged titin is6–M9). (**b**) Proximity ligation assay (PLA) on rat muscle sections. PLA signals (red dots) indicated spatial proximity of DNAJB6 with its known interaction partner HSPA8, and with the CASA complex proteins BAG3, HSPB8, and STUB1. Negative control experiments were performed with DNAJB6 or BAG3 antibodies alone. Each image shows a representative maximum-intensity projection through a Z-stack of 6.4 μm, with the PLA signal (red) superimposed on the phalloidin counterstain (grey). Scale bar, 5 μm. (**c**) Co-injection of *DNAJB6* and *BAG3* in zebrafish. Zebrafish embryos were injected with *DNAJB6b* p.Phe93Leu mRNA and wild-type (wt) or p.Pro209Leu mutant *BAG3* mRNA in indicated combinations. Co-injection of wild-type

BAG3 with mutant *DNAJB6* resulted in a more severe phenotype than mutant *DNAJB6* alone, reflected by a significant increase in class II embryos. In contrast, co-injection of p.Pro209Leu *BAG3* with mutant *DNAJB6b* did not alter the phenotype distribution. Statistical significance (χ^2 test) is denoted by *P* value or n.s. (not significant). Scale bar, approx. 50 μm.

Table 1

DNAJB6 mutation status in affected and unaffected individuals from Finnish (FF), U.S. Caucasian (DUK), and Italian (IT) LGMD1D families

Family ID	Mutation	Affected		Unaffected	
	nucleotide change (protein change)	Total	Mutation carriers	Total	Mutation carriers
FF1	c.279C>G (p.Phe93Leu)	9	9	9	0
FF2	c.279C>G (p.Phe93Leu)	3	3	3	0
FF3	c.279C>G (p.Phe93Leu)	1	1	2	0
FF4	c.279C>G (p.Phe93Leu)	2	2	N/A	N/A
FF5	c.279C>G (p.Phe93Leu)	1	1	N/A	N/A
DUK1047	c.267T>A (p.Phe89Ile)	10	10	11	1*
DUK1701	c.267T>A (p.Phe89Ile)	19	19	22	1*
IT1	c.279C>A (p.Phe93Leu)	8	8	6	0
IT2	c.277T>C (p.Phe93Leu)	4	4	4	0

* Individuals of uncertain affection status. At their most recent exam, these mutation carriers were younger than the oldest age of onset previously identified in their respective families (DUK1047, 55 y; DUK1701, 50 y).